ACS OMEGA

http://pubs.acs.org/journal/acsodf

Article

Biosynthesis of Silver Nanoparticles Functionalized with Histidine and Phenylalanine Amino Acids for Potential Antioxidant and Antibacterial Activities

Gemechu Shumi,* Taye B. Demissie,* Rajalakshmanan Eswaramoorthy, Raji Feyisa Bogale, Girmaye Kenasa, and Tegene Desalegn*

Cite This: *ACS Omega* 2023, 8, 24371−24386

Read Online

ACCESS | Metrics & More | Article Recommendations | Supporting Information

ABSTRACT: Due to biochemically active secondary metabolites that assist in the reduction, stabilization, and capping of nanoparticles, plant-mediated nanoparticle synthesis is becoming more and more popular. This is because it allows for ecologically friendly, feasible, sustainable, and cost-effective green synthesis techniques. This study describes the biosynthesis of silver nanoparticles (AgNPs) functionalized with histidine and phenylalanine using the *Lippia abyssinica* (locally called koseret) plant leaf extract. The functionalization with amino acids was meant to enhance the biological activities of the AgNPs. The synthesized nanoparticles were characterized using UV−Visible absorption (UV−Vis), powder X-ray diffraction (pXRD), scanning electron microscopy (SEM), energy-dispersive X-ray (EDX) spectroscopy, transmission electron microscopy (TEM), and Fourier transform infrared (FTIR) spectroscopy. The surface plasmonic resonance (SPR) peak at about 433 nm confirmed the biosynthesis of the AgNPs. FTIR spectra also revealed that the phytochemicals in the plant extract were responsible for the capping of the biogenically synthesized AgNPs. On the other hand, the TEM micrograph revealed that the morphology of AgNP-His had diameters ranging from 5 to 14 nm. The antibacterial activities of the synthesized nanoparticles against Gram-positive and Gram-negative bacteria showed a growth inhibition of 8.67 ± 1.25 and 11.00 ± 0.82 mm against *Escherichia coli* and *Staphylococcus aureus*, respectively, at a concentration of 62.5 μg/mL AgNP-His. Moreover, the nanoparticle has an antioxidant activity potential of 63.76 ± 1.25% at 250 μg/mL. The results showed that the green-synthesized AgNPs possess promising antioxidant and antibacterial activities with the potential for biological applications.

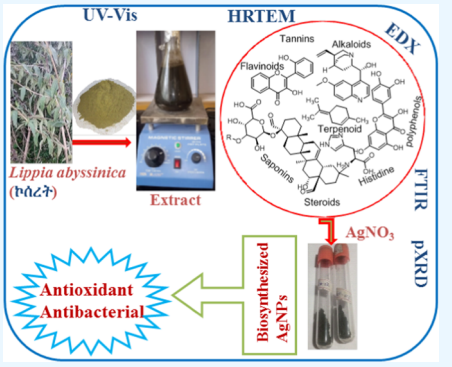

1. INTRODUCTION

The scientific community has paid special attention to the development of metal-based nanoparticles due to their exceptional biological and physicochemical properties and their potential use in a variety of applications for the betterment of human life.[1−3] Among several metal nanoparticles, silver nanoparticles (AgNPs) are the most dynamic and interesting nanomaterials that have gained significant focus in the area of nanotechnology.[4] These particular interests are associated with their unique chemical, physical, and biological characteristics in comparison to bulk size.[5] They possess high thermal and electrical conductivity,[6] surface-enhanced Raman scattering properties, chemical stability, catalytic activity,[7] nonlinear optical behavior,[8] drug delivery, and antimicrobial effects.[9] Owing to their unique properties, AgNPs have been widely applied in many fields, such as shampoos, soaps, detergents,[10] cosmetics,[11] toothpastes, electronics, optics, and medical and pharmaceutical products.[12]

In addition, these materials also have several advantages, including their high surface-area-to-volume ratio, which allows them to attach ligands with different functionalities to develop materials with custom-tailored properties that enhance their toxicity toward pathogens, capacity to kill cancer cells, and efficient catalytic properties.[13] However, the synthesis methods and the materials used for the synthesis of nanoparticles determine the acceptance and utility of the nanoparticles for different applications.[14] The synthesis of metal nanoparticles involves either chemical or biogenic/biological methods, mainly for reducing and capping the metal into nanoparticles/materials.[15] Chemical methods using toxic, hazardous, and expensive organic solvents like citrate ($HOC(CH_2CO_2H)_2$), borohydride $[BH_4]^-$, thioglycerol, and 2-mercaptoethanol to prepare the nanoparticles were reported.[16] However, the use of toxic chemicals during chemical synthesis posed a major concern as they have adverse effects on the environment as well as on living beings.[17] As a result, the need

Received: March 21, 2023
Accepted: June 14, 2023
Published: June 26, 2023

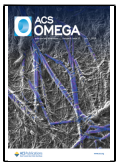

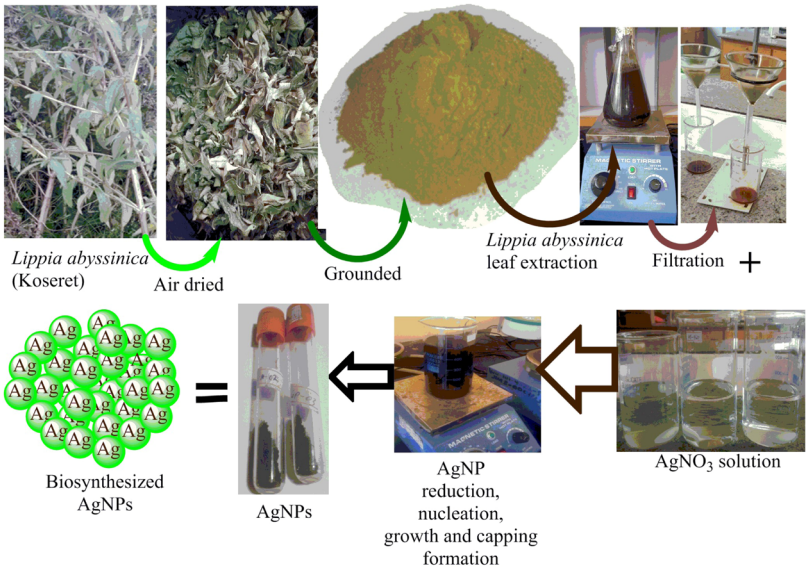

Figure 1. Schematic representation for LALE-mediated biosynthesis of AgNPs.

for technologies that produce nanoparticles using safe and benign processes has increased, shifting focus to biological techniques.[18]

Biogenic synthesis of metal NPs using simple amino acids, sugars, biodegradable polymers, vitamins, and plant phytochemicals has been reported.[19] The biological resources can be used to prepare nanoparticles that are safe for the environment, recyclable, feasible, and useful in both food technology and medicine.[20] Consequently, metabolites, such as terpenoids, alkaloids, polyphenols, phenolic acids, proteins, and sugars, are well known for their reductive activity and hence are responsible for stabilizing and reducing metal ions.[13,21] Related to this, coordination bonding and selective capping agent adsorption on the surface of NPs might cause the NPs to create a bond with the phytocomponents of the plant extract, which helps to prevent nanoparticle aggregation through electrostatic stabilization.[22]

Nowadays, finding an effective formulation to treat microbial infections has become a critical issue due to the emergence of multidrug-resistant bacterial strains, the drugs' low efficiency, and the adverse side effects of conventional antibiotic drugs.[23] As such, the functionalization of nanoparticles through various capping agents is believed to be among the methods leading to the development of new effective drug molecules. The most commonly used agents for the surface functionalization of metal nanoparticles are amino acids.[24,25] The surface functionalization provides additional sites, such as amino or carboxyl groups, to act as a coupling agent between the nanoparticles and biomolecules. This enhances the stability of the nanoparticles and improves their activities.[2,26] Related to this, it has been reported that histidine has the highest antioxidant activity and phenylalanine has a moderate antioxidant activity as compared to other 20 amino acids.[27] Moreover, histidine was also reported to be the most reducing and capping agent,[13,19] whereas tyrosine, tryptophan, and phenylalanine are moderately reducing and stabilizing agents for the synthesis of AgNPs.[28]

In this study, the leaf extract from *Lippia abyssinica* was used as a reducing and capping agent for the green synthesis of AgNPs. In Ethiopia, *L. abyssinica* (Koseret) has been traditionally used as a spice and traditional medicine for analgesic, antipyretic, and antioxidant activities.[29] *L. abyssinica* is rich in flavonoids and has higher free radical scavenging activities than other spices like *Nigella sativa* (Thikur azmud), *Piper capense* (Timiz), *Thymus schimperi* (Tosign), and *Trachyspermum ammi* (Netch azmud).[29] Hence, we hereby report a novel green synthesis of silver nanoparticles using a traditional medicinal plant *L. abyssinica* leaf extract (LALE) as the reducing and capping agent. The synthesized silver nanoparticles were further functionalized with amino acids of different polarities (phenylalanine and histidine) to enhance the bioactivities by decreasing the size of the nanoparticles. The obtained AgNPs were characterized using transmission electron microscopy (TEM), Fourier transform infrared spectroscopy (FTIR), X-ray diffraction (XRD), and UV−Vis spectroscopy and were tested for their antibacterial and antioxidant activities.

2. MATERIALS AND METHODS

2.1. Reagents. All of the chemicals and reagents used in this research were of analytical grade. Silver nitrate ($AgNO_3$, 99.8%, India), ferric chloride ($FeCl_3$, 99% from Loba Chemie, India), Muller-Hinton Agar (MHA, Merck chemical company), chloroform ($CHCl_3$, 99.9%, Fisher Scientific U.K. Limited, U.K.), sulfuric acid (H_2SO_4, 98%), sodium hydroxide (NaOH, 98%), ascorbic acid ($C_6H_8O_6$, 99.9%, Loba Chemie, India), hydrochloric acid (HCl, 37% India), DPPH ($C_{18}H_{12}N_5O_6$, 99%, Sigma-Aldrich, Germany), L-phenylalanine ($C_9H_{11}NO_2$, 98.5%, Loba Chemie, India), and L-histidine ($C_6H_9N_3O_2$, 1.449 g/cm^3 Loba Chemie, India) were used. *L. abyssinica* plant leaves were collected from the Guto Gida district, East Wollega Zone, Oromia, Ethiopia, located 335 km from Addis Ababa at latitude: 9° 04′ 60.00″ N and longitude: 36° 32′ 59.99″ E.

2.2. Plant Material Collection and Preparation. The preparation of *L. abyssinica* extract was conducted using reported procedures with slight modifications.[30] The fresh leaves of *L. abyssinica* were collected and washed with tap water several times, followed by rinsing with double distilled water to remove any dust particles. To get rid of the moisture content in the leaves, it was air-dried in a shadowy environment at room temperature. The dried leaves were

https://doi.org/10.1021/acsomega.3c01910
ACS Omega 2023, 8, 24371−24386

Scheme 1. Proposed Mechanism for the Formation of Functionalized Silver Nanoparticle Using Histidine and Flavonoids

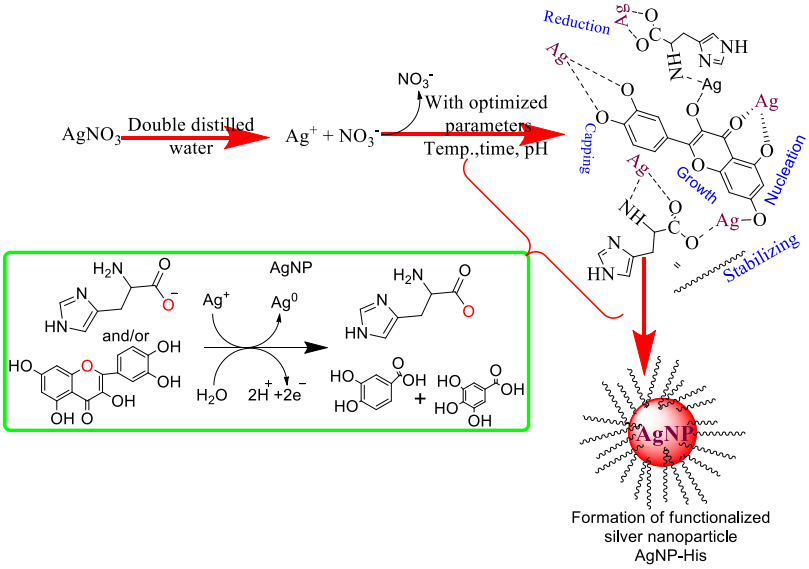

ground into a fine powder using an electric blender. For further use, the powder was packaged and kept at an ambient temperature in a dark space. The extraction was carried out by taking 20 g of the powdered plant leaves in a 500 mL conical flask containing 400 mL of distilled water. It was covered with aluminum foil to prevent the effect of light on the solution. The mixture was stirred for 30 min and then heated at 60 °C with continuous stirring on a hot plate for 1 h. After cooling down to room temperature, the solution was filtered with Whatman No. 1 filter paper to get a clear extract solution, as shown in Figure 1. The filtrate was stored at 4 °C for further experiments.

2.3. Phytochemical Screening. A preliminary phytochemical screening of the aqueous leaf extracts was performed using reported techniques.[31−33]

2.3.1. Phenolic Test. The ferric chloride test method, which involves adding 2 mL of a 5% solution of $FeCl_3$ to 1 mL of *L. abyssinica* leaf extract in a test tube and shaking them together before standing the test tube upright in a rack of test tubes, was the technique used to determine phenol qualitatively. The reaction mixture had a black color, indicating that phenol was indeed present.[31,32]

2.3.2. Alkaloids Test: Mayer's Test. A mixture of 3 mL of *L. abyssinica* leaf extract and 3 mL of 1% HCl solution was heated for 20 min in a water bath. Mayer's test was run using the reaction mixture that resulted after being cooled to room temperature. Drop by drop, 1 mL of Mayer's reagent (1.36% $HgCl_2$ and 5% KI) was added to the reaction mixture after cooling. Alkaloids were present as evidenced by the precipitation of a greenish-colored cream precipitate.[31−33]

2.3.3. Flavonoid Test: Alkaline Reagent Test. 3 mL of LALE was added to 1 mL of a 10% NaOH solution in the test tube. A bright yellow hue was developed, which supports the presence of flavonoids. By dropping diluted HCl, the color gradually vanished.[31,32]

2.3.4. Terpenoid and Steroid Salkowski Test. The test tube was filled with 5 mL of LALE, 2 mL of chloroform, and 3 mL of concentrated sulfuric acid, and it was thoroughly shaken to create a layer. The interface took on a reddish-brown color, indicating the presence of terpenoids. The lower surface is red, indicating the presence of steroids.[31,32]

2.3.5. Tannin Test. 2.3.5.1. Ferric Chloride Test. When 1 mL of distilled water and 2 drops of ferric chloride solution were added to 0.5 mL of LALE in a test tube, a blue-black coloration was noticed, indicating the presence of tannins.[31,32]

2.3.5.2. Lead Acetate Test. When 0.5 mL of LALE in the test tube solution was added to a 10% lead acetate solution, white precipitation was observed, confirming the presence of tannins.

2.3.6. Saponins-Frothing Test. In a test tube, 0.2 mL of the LALE was shaken with 5 mL of distilled water. Saponin was detected through foaming.[31−33]

2.4. Green Synthesis of Silver Nanoparticles. In a typical reaction system, *L. abyssinica* leaf extract (LALE) was added dropwise to a solution of $AgNO_3$ (as a precursor). In a 50 mL volumetric flask, an optimized concentration of the aqueous solution of $AgNO_3$ (2, 4, 8, 12, 16 mM) was made and used for the synthesis of silver nanoparticles. The formation of AgNPs was studied in relation to concentration, reaction time, LALE volume ratio, temperature, and pH. The optimal volume of LALE (1/20 w/v) was combined with the optimal concentration of the $AgNO_3$ solution for the reduction of Ag ions at an optimized temperature and reaction time (80 °C and 2 h). The reaction was carried out in a dark place by using aluminum foil to cover it. The solution was continuously homogenized while being stirred at 10,000 rpm and at a desired temperature. The completion of the reaction was confirmed by the color change observed.[34] A double-beam UV−Vis spectrophotometer was used to measure the reaction progress to optimize the $AgNO_3$ solution concentrations, reaction time, volume ratio of $AgNO_3$ to plant leaves, reaction mixture temperatures, and pH effects. Following the optimization of the reaction conditions, a color change from colorless to brown was noticed, which indicated the formation of silver nanoparticles. The product was separated from the mixture using a high-speed centrifugation for 20 min at 10,000 rpm. Then, the synthesized AgNP pellets were rinsed with 20 mL of distilled water and dried at 105 °C for further characterizations.[30]

2.5. Green Synthesis of Silver Nanoparticles Functionalized with Histidine and Phenylalanine. The synthesis of functionalized silver nanoparticles (f-AgNPs) was

https://doi.org/10.1021/acsomega.3c01910
ACS Omega 2023, 8, 24371−24386

conducted using the reported procedure with slight modification.[35] Briefly, 10 mL of aqueous LALE was added to 2 mM of aqueous solution of $AgNO_3$ in 50 mL of a volumetric flask. Subsequently, histidine or phenylalanine as a surface-modifying agent was added to the reaction mixture slowly drop by drop while stirring on a hot plate, as shown in Scheme 1. The pH of the solution was adjusted to 12.01 using 1 M of NaOH solution. The reaction proceeded for 2 h at 80 °C under constant stirring. Finally, the f-AgNPs were separated from the mixture by high-speed centrifugation at 10,000 rpm for 20 min. After centrifugation, the synthesized f-AgNP pellets were rinsed with 20 mL of distilled water and dried in an oven at 105 °C for further characterizations. Therefore, in the study, two categories of AgNPs were synthesized, namely, non-functionalized AgNPs and amino acid-functionalized AgNPs (f-AgNPs, AgNP-his, and AgNP-phen).

2.6. Characterization of Silver Nanoparticles. *2.6.1. UV−Visible Spectrophotometer Analysis.* Using a double-beam UV−Vis spectrophotometer (Shanghai Drawell Scientific Instrument), the initial physicochemical characterization of the biosynthesized AgNPs, the reduction of silver ions using LALE, and the functionalization with histidine and phenylalanine were examined by UV−Vis in the range of 200−800 nm.

2.6.2. Fourier Transform Infrared Spectroscopy (FTIR) Analysis. FTIR spectrometer (PerkinElmer Spectrum 65 FTIR Spectrometer) was used to conduct the FTIR spectral analysis. The FTIR spectra were collected at the standard spatial resolution in the transmission mode between 4000 and 400 cm^{-1}. The samples were made using the KBr pellet technique, and they were examined to see if the organic functional groups were connected to the surface of AgNPs, which are the agents for reduction, stabilization, and capping.[36]

2.6.3. X-ray Diffractometer (XRD) Analysis. An X-ray diffractometer (Shimadzu Corporation (Japan); XRD-7000 X-ray diffractometer) was used for the XRD analysis to study the crystallographic nature of the biosynthesized AgNPs. The Cu Kα radiation source was used with a wavelength of 1.5406 Å and a scanning angle of 2θ in the scattering range of 10−90° on an instrument operating at a voltage of 45 kV and a current of 40 mA.

2.6.4. Scanning Electron Microscope (SEM) with Energy-Dispersive X-ray (EDX) Analysis. The oven-dried AgNP-his was loaded onto the stub with a carbon tape fixed and coated by sputtering with gold. The prepared sample was investigated to determine the morphology of AgNP-his and characteristics of the elemental analysis of AgNP-his with the help of a scanning electron microscope (SEM) EVO18 (CARL ZEISS) and an energy-dispersive X-ray-spectrometer Quanta 200 with X Flash 6130.

2.6.5. Transmission Electron Microscope (TEM) Analysis. Transmission electron microscopy (TEM, HF5000, Hitachi High-Technologies, Japan), which operates at 200 kV and is equipped with an energy-dispersive system (EDS), was used. High-resolution transmission electron microscopy (HR-TEM) technology, resolution: 0.14 nm lattice, 0.12 nm point-to-point, magnification range: 4000×−15,000,000×, high dispersion diffraction camera length range: 4−80 m. Specimen tilt range: +/−20° (for UHR configuration), +/−30° (for HR and HC configurations). TEM images of AgNPs were processed with the ImageJ software to obtain the diameter size distribution of the particles.

2.7. Biological Activities of the Biosynthesized AgNPs. *2.7.1. Antibacterial Study.* Antibacterial activities of biosynthesized AgNPs were conducted on Mueller Hinton agar media by agar-well diffusion method adapting a reported procedure.[37] 1 mL of actively growing clinically strains of *Staphylococcus aureus* ATCC 25926 and *Escherichia coli* ATCC 25922 (obtained from Ethiopian Public Health Institute, which contain approx. 1×10^7 CFU mL^{-1}, 0.5 McFarland Standard) were uniformly spread plate on agar media using cotton swabs. Wells were made in each agar culture media using a sterile cork borer (6 mm in diameter) and were filled with 100 mL of AgNPs (62.5 μg/mL, 2 mM of the green-synthesized AgNP, AgNP-his, and AgNP-phen), dimethyl sulfoxide (DMSO as a negative control), and gentamicin (positive control) in triplicate. After preserving it in the refrigerator for 30 min, the culture media were incubated at 37 °C for 24 h. Finally, the zones of inhibition were recorded as the diameter of the growth-free zones measured in mm using a Vernier caliper.[38]

2.7.2. Antioxidant Activity Study. A standard procedure was followed to test the antioxidant activity of the biogenically synthesized AgNPs.[39] From a 50 mg/mL stock solution, separate test tubes containing various concentrations of synthesized AgNPs and standard ascorbic acids (50, 100, 150, 200, and 250 μg/mL) were prepared. 3 mL of a 0.1 mM methanolic solution DPPH was then added to each prepared solution, and the test tubes were left to incubate for 20 min in the dark. After incubation, the absorbance of the solutions was measured at 517 nm against methanol as a blank using a double-beam UV−Vis spectrophotometer. 0.2−1.0 mg/mL of ascorbic acid in methanol was used as the standard. During analysis, the experiment was performed in triplicate for statistical analysis. The following formula eq 1 was used to calculate the antioxidant activity in terms of the percent activity

$$\text{percent activity}\ (\%) = [(A_c - A_s)/A_c] \times 100 \quad (1)$$

where A_c is the absorbance of control and A_s is the absorbance of the silver nanoparticle solution (AgNP).

2.8. Statistical Data Analysis. One-way analysis of variance (ANOVA) was used to compare the mean antimicrobial and antioxidant properties of the synthesized AgNPs using the Statistical Analysis Software (SAS 14.1) at a 5% probability.

3. RESULTS AND DISCUSSION

3.1. Phytochemical Analysis of the Plant Leaf Extract. In this study, a biogenic synthesis of nanoparticles employing a bottom-up method has been carried out using phytochemicals extracted from *L. abyssinica* that might act as reducing and

Table 1. Preliminary Phytochemical Screening Profile of the LALE[a]

s.n	metabolites	test response	methods
1	phenol	+	ferric chloride test
2	flavonoids	+	alkaline reagent test
3	saponins	+	frothing test
4	tannins	+	ferric chloride test
			lead acetate test
5	terpenoids and steroid	+	Salkowski test
6	alkaloids	+	Mayer's reagent test

[a]+ Present.

https://doi.org/10.1021/acsomega.3c01910
ACS Omega 2023, 8, 24371−24386

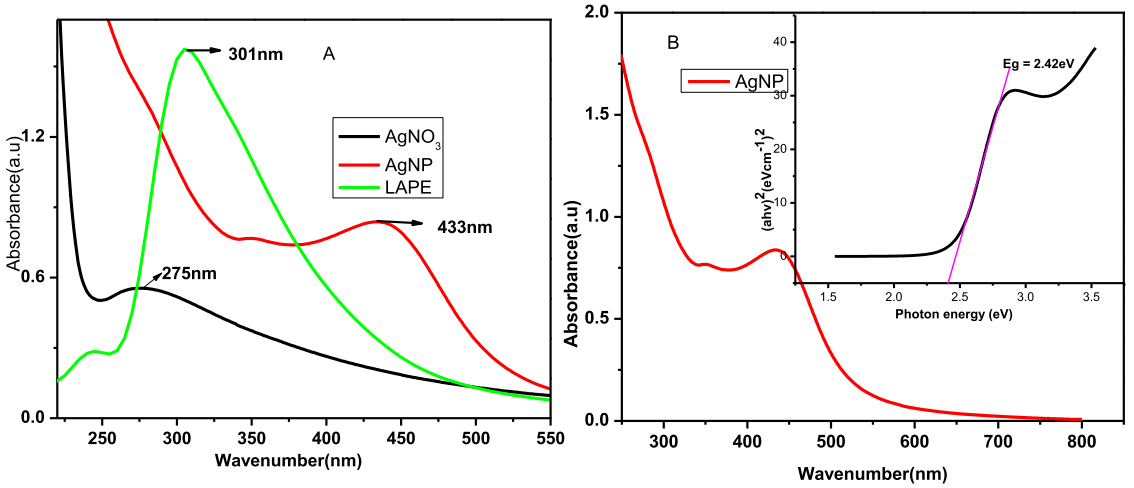

Figure 2. UV−Visible spectra of (A) $AgNO_3$, LALE, and AgNP formed using LALE and (B) band gap of the biosynthesized AgNP.

stabilizing agents in the process.[40] The phytochemical composition of LALE was analyzed qualitatively using the standard procedure to determine the presence of some phytoconstituents in the leaf extract of the medicinal plant. The confirmatory test, which involves color changes, precipitate formation, and others, was used to determine the presence or absence of useful bioactive ingredients such as alkaloids, tannins, flavonoids, flavones, terpenoids, phenols, and saponins in leaf extracts. The phytoconstituents' characteristics of the LALE are summarized in Figure S1 and Table 1. According to the findings, phenols, terpenoids, flavonoids, alkaloids, terpenoids, steroids, and saponins were present in the aqueous extract of the leaves of *L. abyssinica*. The results are in agreement with previously reported results.[41−43] The synthesis of the nanoparticles was significantly influenced by the presence of these bioactive components, which potentially serve to reduce, cap, and stabilize them, minimizing the chances of agglomeration.

3.2. Silver Nanoparticle Synthesis. The syntheses of AgNPs were carried out under optimized conditions using LALE as a reducing and capping agent. On adding the leaf extract, the colorless silver nitrate solution turned into a deep brown solution as shown in Figure 1. This is in agreement with previous studies on silver nanoparticles synthesized using different plant extracts.[15,34,44] The reaction mixture's change in color was considered the strongest indication that AgNPs had been formed. Additionally, the optical characteristics of AgNPs contributed to color variations. This was due to surface plasmon resonance (SPR) peaks, the unique characteristic property observed when free-moving electrons of AgNPs interact with UV or visible radiation.[70]

The mechanism of the AgNP synthesis could be explained by the electron-donating capacity of the plant extract's biomolecule content (polyphenols, alkaloids, saponins, tannins, terpenoids, and flavonoids) resulting in the reduction of Ag^+ ions to the Ag metal. In addition, the synthesized AgNPs were stabilized by the bioactive compounds' functional groups like carbonyl or hydroxyl (alcohol) that keep them from agglomeration. For example, the hydroxyl groups in saponins interact with the Ag^+ ions to form AgNPs and provide stability for the newly formed nanoparticles. Saponins present in the plant extract might also interact with the Ag^+ ions through their hydroxyl groups.[45] By interacting with the metallic ions through the extract's carbonyl functional groups, flavonoids release reactive hydrogen, which then changes the flavonoid's enol into keto form, resulting in the formation of Ag^0.[46] The illustration in Figure S2 shows some proposed bioreduction mechanisms of AgNPs by phytochemicals.

3.3. Characterization of Synthesized Silver Nanoparticles. *3.3.1. UV−Vis Spectroscopy.* UV−Vis spectroscopy was used to monitor the bioreduction of silver ions to AgNPs. The size, shape, and production of the AgNPs in aqueous suspensions can be determined using UV−Vis spectroscopy.[47] The absorbance in the scanning range of 200−800 nm was measured to track the formation and determine the optimized parameters for the synthesis of the AgNPs. Metallic nanoparticles have characteristic optical absorption spectra in the UV−Vis region. Electrons are limited to specific vibration modes by the particle's size and shape. The dispersions of silver nanoparticles showed an intense band due to the SPR absorption. The surface of a metal is like plasma, having free electrons in the conduction band[48] and positively charged nuclei. SPR is a collective excitation of the electrons in the conduction band near the surface of the nanoparticles. The band gap of the synthesized silver nanoparticle from (Figure 2) was estimated to be about 2.45 eV, which is comparable to previously reported results.[49]

The appearance of a typical SPR peak between 400 and 500 nm[50] further supported the color change, indicating that AgNPs were formed. As shown in Figure 2, the SPR peaks of $AgNO_3$, LALE, and AgNP were 275, 301, and 433 nm, respectively. These results are also in good agreement with literature reports confirming that AgNP was formed.[51] The absorbance band maxima of AgNP appeared in the range of 400−450 nm due to the surface resonance of AgNPs.[52] This is also in good agreement with previously reported results using different plants, for instance, AgNP synthesis with *Solanum trilobatum* (430 nm),[53] *Cinnamomum tamala* (416 nm),[54] and *Eichhornia Crassipes* (450 nm).

Various variables, including time, temperature, pH, the volume of LALE, and silver nitrate concentration influenced the biosynthesis of AgNPs during optimization. Accordingly, LALE, which was employed as a capping and reducing agent, helped to make it possible to observe the peak of the AgNP formed at a red shift (bathochromic) compared to the precursors ($AgNO_3$ and LALE in Figure 2A). Related results

https://doi.org/10.1021/acsomega.3c01910
ACS Omega 2023, 8, 24371−24386

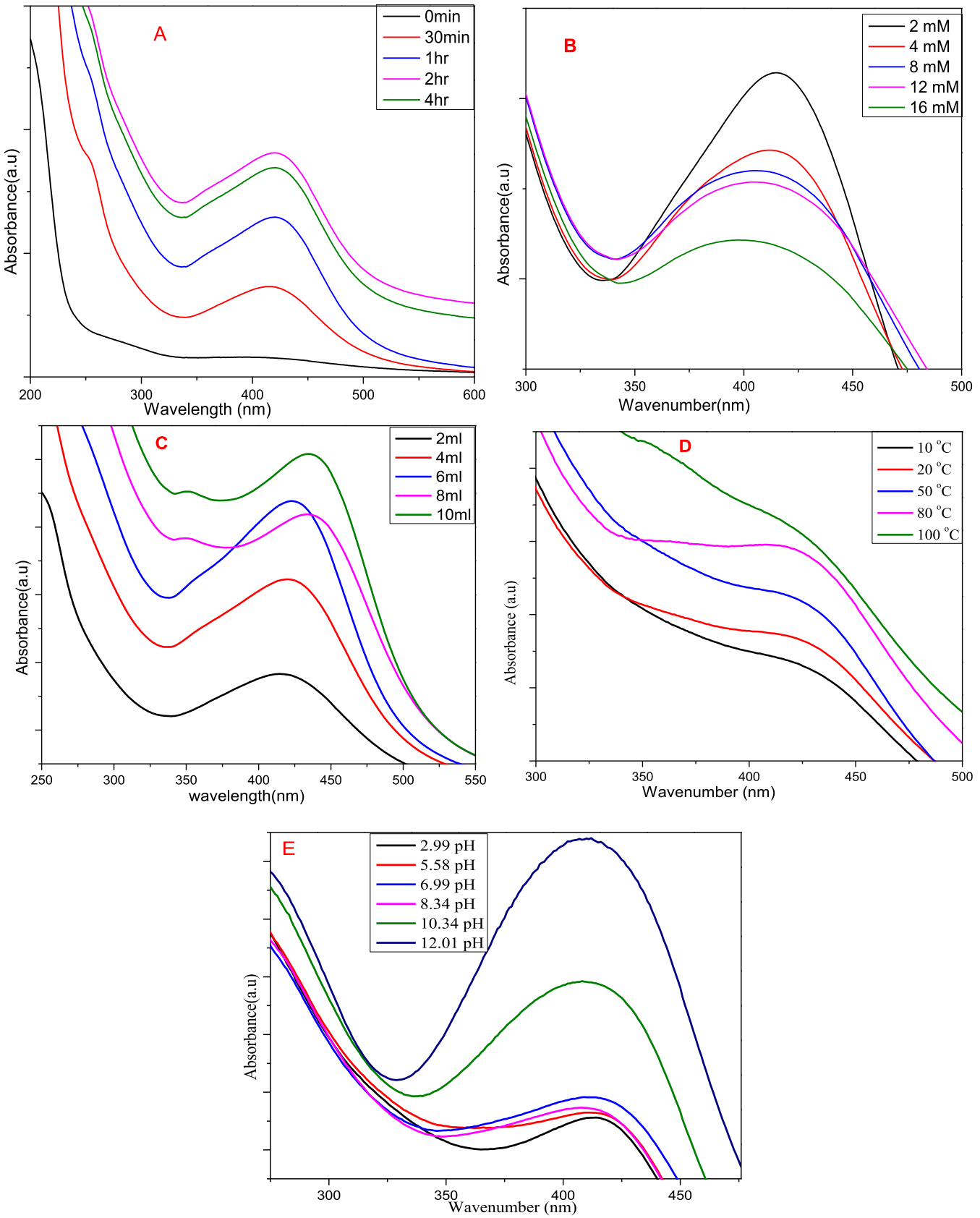

Figure 3. Surface plasmon resonance spectra of biosynthesized AgNPs recorded as a function of (A) time, (B) concentration of $AgNO_3$ solution, (C) concentration of extract, (D) temperature, and (E) pH effect.

were also reported using *Abelmoschus esculentus* plant extract as a bioreduction agent for the synthesis of silver nanoparticle.[55]

3.3.2. Optimization Parameters Using UV−Vis Spectroscopy for the Synthesis of AgNPs. 3.3.2.1. Influence of $AgNO_3$

https://doi.org/10.1021/acsomega.3c01910
ACS Omega 2023, 8, 24371−24386

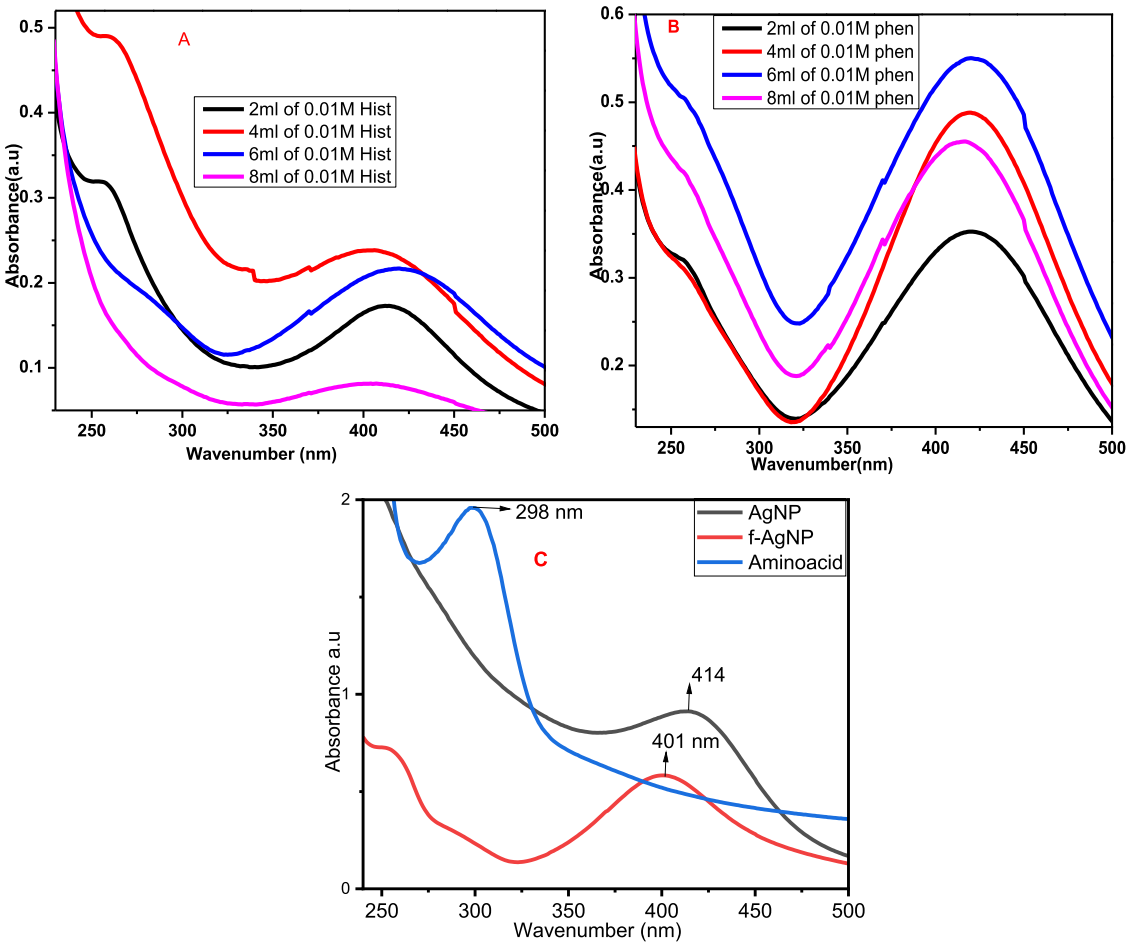

Figure 4. Optimization of the volume of 0.01 M of (A) histidine and (B) phenylalanine for functionalization of the green AgNP synthesis and (C) comparison of f-AgNP with others.

Concentration on the Biosynthesis of AgNPs. The silver ion concentration optimization was done by taking 2, 4, 8, 12, and 16 mM. The changes in the reactions were monitored by UV−Vis spectroscopic scanning, and the spectra were recorded (Figure 3B). The production rate increased with a decrease in the $AgNO_3$ concentration. The UV−Vis spectral data revealed that the optimum concentration of $AgNO_3$ was 2 mM, above which the product quantity started to decline; hence, at a higher concentration of $AgNO_3$, the absorbance was found to decrease and shift to blue (from 416 to 397 nm), in agreement with a previous study.[56]

3.3.2.2. Effects of Volume Ratio of $AgNO_3$ to LALE. In the case of $AgNO_3$ to LALE ratio optimization (Figure 3C), the absorption spectra of AgNPs obtained changed with the volume of LALE as 2, 4, 6, 8, and 10 mL extracts. With the increase in the concentration of LALE in the reaction mixture (1:5), the peak intensity increases abruptly, indicating an enhancement in the production of AgNPs.[57] Additionally, as LALE volume increased, the absorption spectrum slightly shifted toward a longer wavelength region (from 414 to 434 nm), indicating that AgNP size had increased as the spectra shifted to red.[57]

3.3.2.3. Effects of Temperature on the Synthesis of AgNPs. To optimize the reaction temperature, each reaction was run independently for 2 h at various temperatures (10, 20, 50, 80, and 100 °C). UV−Vis spectroscopy was used to measure the absorbance of the resulting solutions as shown in Figure 3D. At a temperature of 80 °C, nanoparticles of good stability and high yield were obtained. As a result, in this study, the optimum temperature for the AgNP synthesis was 80 °C.

3.3.2.4. Reaction Time Influences on the Synthesis of AgNPs. The reactions for the phytomediated synthesis of nanoparticles were carried out at various time intervals ranging from 0 to 4 h. As shown in Figure 3A, the absorption spectra were scanned after 0, 30 min, 1, 2, and 4 h. At 2 h, the maximum absorbance was recorded. The results showed that lower absorption peaks at 0, 30 min, and 1 h indicate lower AgNP yields, reaction rates, and stability. With increasing time, the absorbance has increased, which suggests that the formation of AgNPs has improved. As a result, 2 h was considered as the ideal time for the AgNP synthesis, which served as the foundation for additional optimization.

3.3.2.5. Influence of pH on the Green Synthesis of AgNPs. The effect of pH on the reaction for the biosynthesis of silver nanoparticles has been studied at pH values of 2.99, 5.58, 6.99, 8.34, 10.34, and 12.01 at 2 h using UV−Vis spectroscopy (Figure 3E).

The biosynthesis of nanoparticles at pH 2.99, 5.58, 6.99, and 8.34 was slower, as depicted in the absorption spectra. At pH 12.01, high absorption spectra were recorded, indicating that the formation of AgNP was successful and the AgNP was stable, resulting in high yield. The synthesis of the AgNPs was carried out under optimized conditions of 2 mM of $AgNO_3$, a 1:5 metal salt to LALE concentration ratio, a temperature of 80

https://doi.org/10.1021/acsomega.3c01910
ACS Omega 2023, 8, 24371−24386

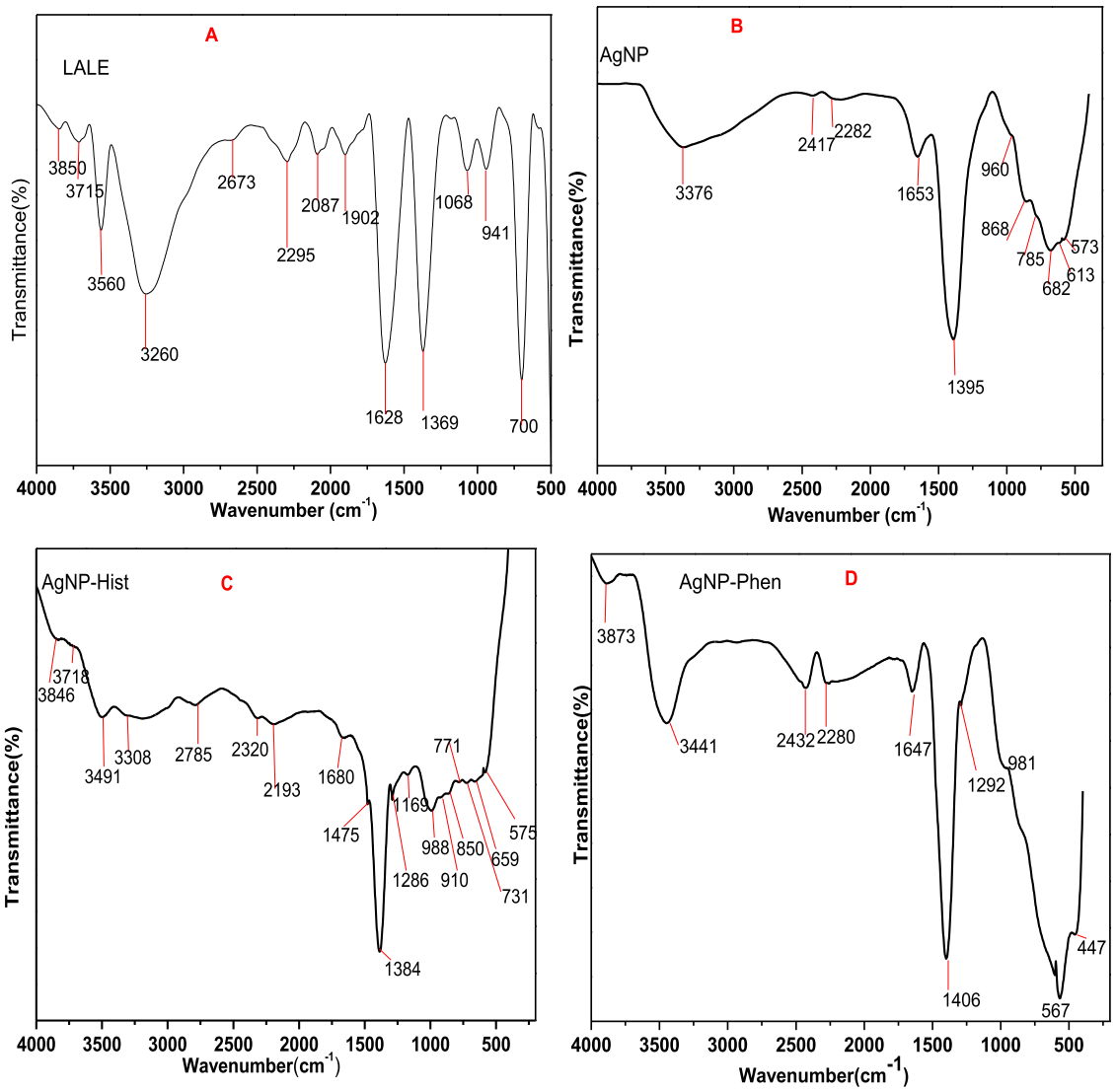

Figure 5. FTIR spectra of *L. abyssinica* leaf extract (LALE (A)), biosynthesis of AgNP (B), biosynthesis of AgNP functionalization of histidine amino acid (AgNP-Hist (C)), and biosynthesis of AgNP functionalization of phenylalanine amino acid (AgNP-Phen (D)).

°C, a time of reaction of 2 h, and a pH of 12.01. These conditions were considered suitable for the biosynthesis of the AgNPs.

3.3.2.6. Functionalization of the Biosynthesized AgNPs Using Amino Acids. The use of NPs for drug design systems (DDSs) can improve the side effects observed in existing pharmacological treatments through the functionalization of NPs for specific targets.[58] The physicochemical features of NPs, such as size, shape, surface charge, surface properties, and conjugation with specific biological molecules, are used to improve the delivery of drugs to the target tissue in two diverse ways: passive and active targeting.[59] In this research, we have functionalized the biosynthesized AgNP with histidine and phenylalanine amino acids. The optimization was done for 0.01 M histidine and/or phenylalanine volume by taking 2, 4, 8, and 10 mL for both amino acids. The UV−Vis spectral data were recorded for each volume at 2 h, a 1:5 volume ratio of $AgNO_3$ to LALE, 80 °C, and pH 12.01. As seen in Figure 4A,B, the 4 and 6 mL of histidine and phenylalanine, respectively, displayed significant absorption peaks, confirming the formation of stable functionalized AgNPs. The biosynthesized AgNPs functionalized with the amino acid absorbance peak shifted to blue, indicating that it increased the surface area and decreased the size of the biosynthesized AgNP (Figure 4C).

3.3.3. Fourier Transform Infrared (FTIR) Spectroscopy Analysis of the AgNPs. FTIR analysis was carried out to obtain information about functional groups present in the AgNPs and understand the transformation of functional groups due to the reducing process. FTIR scanning data were collected between 4000 and 400 cm^{-1}.[60] The functional groups present in biogenically synthesized AgNP and functionalized histidine and phenylalanine were evaluated using FTIR, and the FTIR spectra are presented in Figure 5 and Table 2.

The spectrum of LALE shows absorbance peaks at 3850, 3715, 3560, and 3260 (O−H stretching),[61] 2673, 2295, 2087, 1902, and 1628 (C═O, flavonoids), and 1369, 1068, 941, and 700 cm^{-1} (flavonoids).[62] The spectrum of nonfunctionalized AgNP showed absorbance peaks at 3376, 2417, 2282, 1653, 1395, 960, 868, 785, 682, 613, and 573 cm^{-1}. On the other hand, the spectrum of functionalized AgNP-his showed absorbance peaks at 3846, 3718, 3491, 3308, 2785, 2320, 2193, 1680, 1475, 1384, 1286, 1169, 988, 910, 850, 771, 731, 659, and 575 cm^{-1}, whereas functionalized AgNP-phen showed absorbance peaks at 3873, 3441, 2432, 2280, 1647,

https://doi.org/10.1021/acsomega.3c01910
ACS Omega 2023, 8, 24371−24386

Table 2. FTIR Data Interpretation for Silver Nanoparticles Synthesized

LALE (cm^{-1})	AgNP (cm^{-1})	AgNP-hist (cm^{-1})	AgNP-phen (cm^{-1})	tentative interpretation of the functional group
3850		3846	3873	medium O−H stretching alcohol
3715		3718		medium O−H stretching alcohol
3560	3376	3491	3441	aromatic secondary amine, NH stretch
3260		3308		O−H stretching alcohol
		2785		methylamino, N−CH_3, C−H stretch
2673	2417		2432	thiols (SH stretch)
2295	2282	2320	2280	C≡C C≡ N
2087		2193		C≡C C≡ N
		1680		amide
1628	1653		1647	alkenyl C═C stretch, aryl-substituted CC, conjugated CC, secondary amine, NH bend, CO flavonoid
		1475	1408	methyl C−H asyn./sym-bend, aromatic ring stretch
1369		1384		C−H di, tri, tetramethyl multiplate
			1292	Ar. primary amine, C−N stretch, C−O alcohol, phenol
		1169		C−N stretch, C−O alcohol
1068				cyclohexane ring vibration, C−O alcohol
941	960	988, 911	954	vinyl −CH═CH_2
	868	850	840	aromatic C−H out-of-plane bend
700	785	771, 731		aromatic C−H out-of-plane bend
	682	659		O bonding with metal (with AgNP)
	613		615	O bonding with metal (with AgNP)
	573	575	567	O bonding with metal (with AgNP)

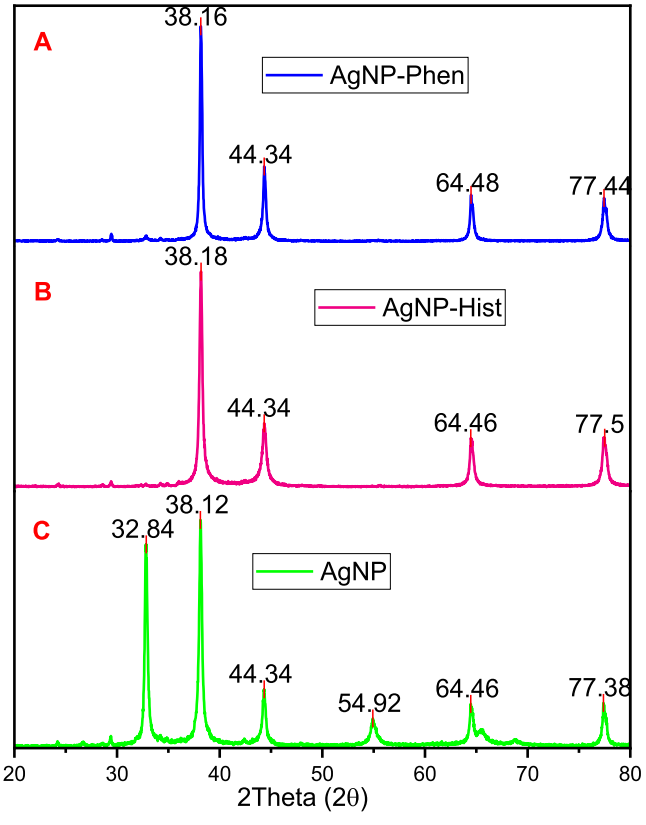

Figure 6. pXRD analysis of biosynthesized and phenylalanine-functionalized AgNP-phen (A), biosynthesized and histidine-functionalized AgNP-his (B), and biosynthesized AgNP (C) without amino acids.

1408, 1292, 954, 840, 615, 567, and 447 cm^{-1}. The spectrum data showed the presence of the biomolecules, and there is some peak shifting between LALE and the synthesized nanoparticles, indicating that LALE served as a capping agent and stabilizer for the synthesis of AgNPs. When compared to the FTIR spectrum of LALE, significant shifts for AgNPs were seen in the regions 1700−1500 and 3600−3100 cm^{-1}, indicating the presence of carbonyl, carboxyl, hydroxyl, and amino groups at their surface, which served to reduce Ag^+ to AgNPs because of their oxidation−reduction potentials. New peaks in a region 600−400 cm^{-1} were also observed due to the formation of AgNP new bonds with oxygen of carbonyl or carboxyl functional groups as a result of the presence of the biomolecules.[63]

Table 3. Average Crystal Size of the AgNPs Was Calculated from XRD Spectra

major peak of AgNPs		2θ (deg)	FWHM (radian)	D (nm)	average D (nm)
major peaks of AgNP	1	32.85	0.3093	26.7774	26. 64
	2	38.14	0.3052	27.5414	
	3	44.32	0.3350	25.6059	
major peaks of AgNP-hist	1	38.19	0.3160	26.6029	25.63
	2	44.34	0.4356	19.6938	
	3	64.51	0.3072	30.5796	
major peak of AgNP-phen	1	38.19	0.2450	34.3134	34.29
	2	44.37	0.2651	32.3625	
	3	64.51	0.2596	36.1870	

3.3.4. X-ray Diffraction Pattern Analysis. Analysis of the crystalline nature of the silver nanoparticle was performed using powder X-ray diffraction spectroscopy. For the measurements, a small amount of dried powder was glued to the nylon loop using highly viscous oil and placed in the center of the pXRD goniometer. The recorded diffractograms are presented in Figure 6. Three crystallographic systems for nonfunctionalized silver nanoparticles (AgNPs), silver nanoparticle-functionalized histidine (AgNP-his), and silver nanoparticle-functionalized phenylalanine (AgNP-phen) were obtained. The pXRD diffraction peaks of the NPs were almost the same as the AgNP diffraction peaks with 2θ values of 32.84, 38.18; 44.34; 54.92, 64.46, and 77.38°, which correspond to

https://doi.org/10.1021/acsomega.3c01910
ACS Omega 2023, 8, 24371−24386

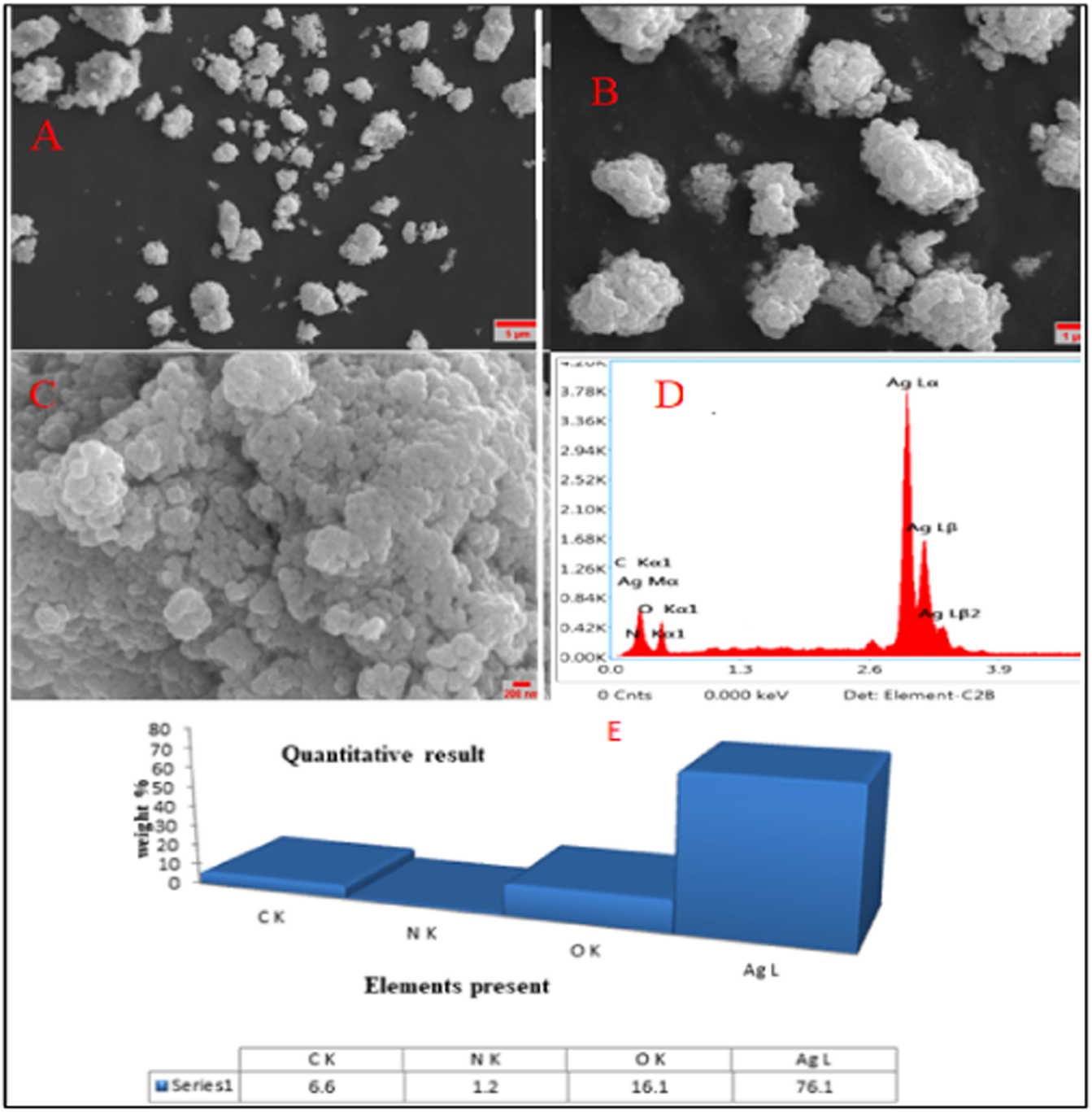

Figure 7. SEM micrograph images of synthesized AgNP-H at different magnification scales (A) 5 μm, (B) 2 μm, (C) 200 nm, and (D and E) EDAX graph and elemental composition.

the planes' *hkl* according to the Miller nomenclature: (110) (111), (200), (220), and (311). The pXRD data closely matched JCPDS No. 00-041-1104 and JCPDS Card No. 04-0783, which describe the cubic structural system of Ag/Ag_2ONPs.[64,68] The AgNP-hist diffraction peaks were identified at the angle values 38.18; 44.34; 64.46, and 77.5°, which is equivalent to the following planes' *hkl*: (111), (200), (220), and (311), and the AgNP-phen diffraction peaks were identified at the angle values 38.16; 44.34, 64.48, and 77.44°, which corresponds to the following planes' *hkl*: (111), (200), (220), and (311). These closely resemble JCPDS card No. 04-0783, which defines the cubic structural system of AgNPs.[52]

According to the pXRD diffractogram analysis, AgNPs were found to be crystalline and contain silver ions. Besides, the peak near 32.85° (110) implied the possible existence of Ag_2O.[64,65] Ag ions (salt) were converted to silver(I) oxide, whereas by significantly increasing the pH of the medium during the biosynthesis of silver nanoparticles, Ag^+ can be converted to silver(I) oxide due to NaOH (aq) used for the pH adjustment. The use of NaOH to produce a solid Ag_2O phase was previously reported[66,67] that silver ions in the presence of OH ions form AgOH (aq), which quickly decompose when heated and precipitate to form the desired Ag_2O,[68] as shown in the following chemical reaction eq 2. Conversely, the use of amino acids (phenylalanine and

https://doi.org/10.1021/acsomega.3c01910
ACS Omega 2023, 8, 24371−24386

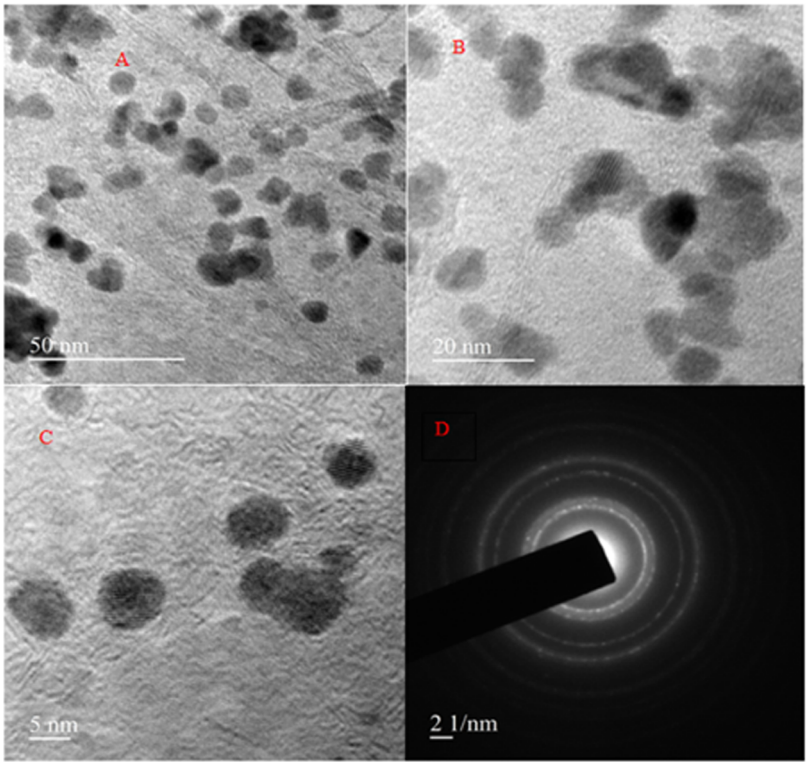

Figure 8. TEM micrograph images of synthesized AgNP-his at different magnification scales (A) 50 nm, (B) 20 nm, (C) 50 nm, and (D) SAED pattern.

histidine) as reducing and capping agents has significantly supported the Ag^+ to Ag° reduction (Figure 6A,B)

$$2Ag(aq)^+ + 2OH(aq)^- \rightarrow Ag_2O(s) + H_2O(l) \quad (2)$$

The average crystal size of the nanoparticles was computed from selected major peaks using the Debye−Scherrer's formula ($D = (k\lambda/\beta \cos\theta)$), where D represents the crystalline size (nm), λ indicates the wavelength of X-rays (0.1541 nm), β specifies the angular line full width at half-maximum (FWHM) of the peak (in radians), and θ displays the Braggs angle (in degrees).[69] The crystalline size of the biosynthesized AgNPs was found to be 26.64, 25.63, and 34.29 nm for the green synthesis of AgNP, AgNP-his, and AgNP-phen, respectively (Table 3).

3.3.5. Scanning Electron Microscopy and Energy-Dispersive X-ray Analysis. The surface morphology of the biosynthesized AgNPs was examined using scanning electron microscopy (SEM). A spherical-like shape of AgNPs was obtained using LALE and histidine (Figure 7C). The results of the energy-dispersive X-ray (EDX) analysis are shown in Figure 7D,E. Figure 7E illustrates the presence of elements including Ag, O, C, and N, with the amount of Ag being the highest (79.1%). The synthesized silver nanoparticles exhibited strong absorption in the 2.5−4 keV range. Metallic silver nanoparticles showed a typically strong signal peak at about 3 keV due to surface plasmon.[70] These results are in agreement with previously reported results using *Pedalium nurex*,[70] *Aloe vera*, and *Curcumin sativus* leaf extracts.[37]

3.3.6. Transmission Electron Microscopy (TEM) and HR-TEM Analysis. Transmission electron microscopy (TEM) was employed to characterize the shape, size, and morphology of the biosynthesized silver nanoparticle functionalized using histidine (AgNP-his). The TEM images of AgNP-his synthesized by LALE are shown in Figure 8A−D. The morphology of AgNP-his is spherical, as confirmed by the SEM. AgNP-his sizes ranged from 5 to 14 nm. The difference in particle size revealed by TEM may be due to aggregation during sample preparation. The crystalline nature of AgNP-his was confirmed by the SAED pattern, which consisted of bright circular spots (Figure 8D). Spots inside the circles correspond to the interplanar distances related to the 111, 200, 220, and 311 planes of the face-centered cubic crystalline structure of the silver nanoparticles, which were confirmed by pXRD results in this study and related results previously reported.[71−73] Also, the lattice space was computed using HR-TEM, and the d-space value was about 0.382 nm, as shown in Figure 9.

3.4. Biological Activities of the Biosynthesized AgNPs. *3.4.1. Antibacterial Studies of the Green-Synthesized AgNPs.* As shown in Table 4, the biosynthesized silver nanoparticle and its histidine- and phenylalanine amino acid-functionalized AgNPs showed inhibition against both the Gram-positive and Gram-negative bacterial pathogens. Particularly, AgNP-his showed the maximum zone of inhibition (11.00 ± 0.82 mm) against *E. coli* ATCC 25922, which was significantly higher as compared to the other nanoparticles (Table 4).

The green-synthesized AgNPs were proven to have different applications including antibacterial properties, although the antibacterial activities of the nanoparticle functionalized with histidine and phenylalanine are not yet reported. Silver nanoparticles synthesized with extracts of*Eucalyptus camaldulensis* and*Terminalia arjuna* showed a zone of inhibition with 16 mm in diameter. The inhibition was significantly higher on Gram-positive bacteria than on Gram-negative bacteria.[74] However, the present results showed that AgNP functionalized

https://doi.org/10.1021/acsomega.3c01910
ACS Omega 2023, 8, 24371−24386

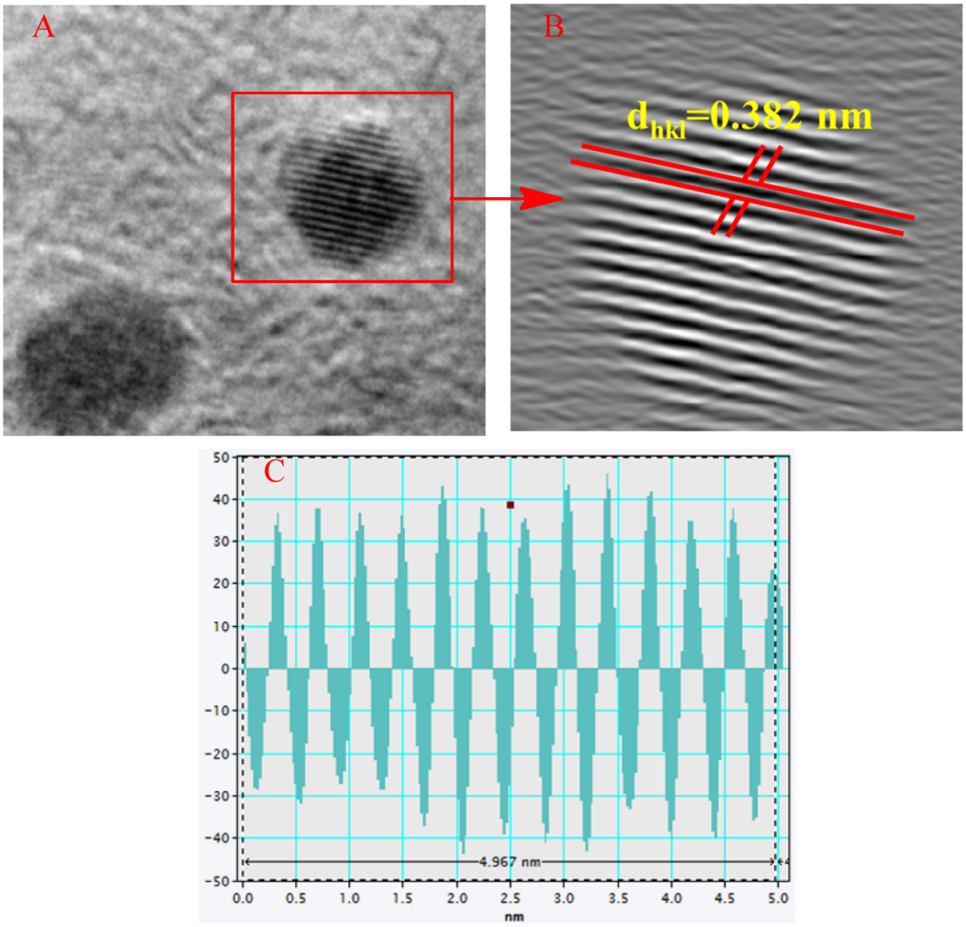

Figure 9. HR-TEM micrograph images of synthesized AgNP-his grain bounder (A), lattice spacing (B), number of peak selected (C).

Table 4. Antimicrobial and Antioxidant Activities of 62.5 μg/mL of 2 mM $AgNO_3$ of Green-Synthesized Silver Nanoparticles and Functionalized with Histidine and Phenylalanine[a]

	antibacterial activities (zone inhibition diameter, mm)		
treatments	*S. aureus* ATCC 25926	*E. coli* ATCC 25922	antioxidant absorbance (%) 250 μg/mL
AgNP	8.00 ± 0.82^{e}	8.67 ± 0.47^{e}	50.29 ± 1.79
AgNP-his	8.67 ± 1.25^{e}	11.00 ± 0.82^{d}	63.76 ± 1.25
AgNP-phen	8.33 ± 0.47^{e}	8.33 ± 1.25^{e}	54.32 ± 1.21
gentamycin (positive control)	22.33 ± 0.47^{a}	20.67 ± 0.47^{ab}	
DMSO (negative control)	nd	nd	

[a]Inhibition zones (mm) designated by the different letters across rows and columns are significantly different from each other at $\alpha = 0.05$ for antibacterial activities.

with histidine was the highest and showed significantly higher activity against the Gram-negative bacteria (*E. coli*). Of course, the antibacterial activity and mechanism of inhibition depend on the type of the species/strain of bacteria, the nanoparticles, concentration, method of synthesis, particle size, shape, and specific surface area.[75]

3.4.2. Antioxidant Studies of Green-Synthesized and Functionalized AgNPs. The green-synthesized AgNP, AgNP-his, and AgNP-phen have shown DPPH free-radical scavenging activity (antioxidant properties). The maximum scavenging activity was for AgNP-his (63.76 ± 1.25%) at a concentration of 250 μg/mL followed by AgNP-phen and AgNP with 54.32 ± 1.21 and 50.29 ± 1.79%, respectively, at the same concentration (Table 4). The results also revealed that the antioxidant activity of the green-synthesized AgNP, AgNP-his, and AgNP-phen increased with an increase in concentration. However, the nanoparticles showed lower activity than ascorbic acid (the positive control) (Figure 10). Previous reports also showed the antioxidant potential of Ag nanoparticles and the enhancement of the properties with amino acid functionalization, particularly with histidine.[76]

4. CONCLUSIONS

A novel green synthetic approach was used to biosynthesize AgNPs using the*L. abyssinica* leaf extract. The biosynthesized AgNPs were further functionalized with histidine and phenylalanine to enhance the biological activities of the nanoparticles. The UV−Vis analysis supports the distinctive peak obtained for the synthesized AgNPs in the 400−450 nm range. FTIR analysis identified the biologically significant active ingredients in the*L. abyssinica* leaf extract and the amino acids responsible for reducing the silver ion. The pXRD analysis corroborated the crystalline nature of the particles, and the average crystallite sizes of AgNP, AgNP-his, and AgNP-phen were found to be 26.64, 25.63, and 34.24 nm, respectively, with a face-centered cubic crystal structure of the silver nanoparticle. The pXRD

https://doi.org/10.1021/acsomega.3c01910
ACS Omega 2023, 8, 24371−24386

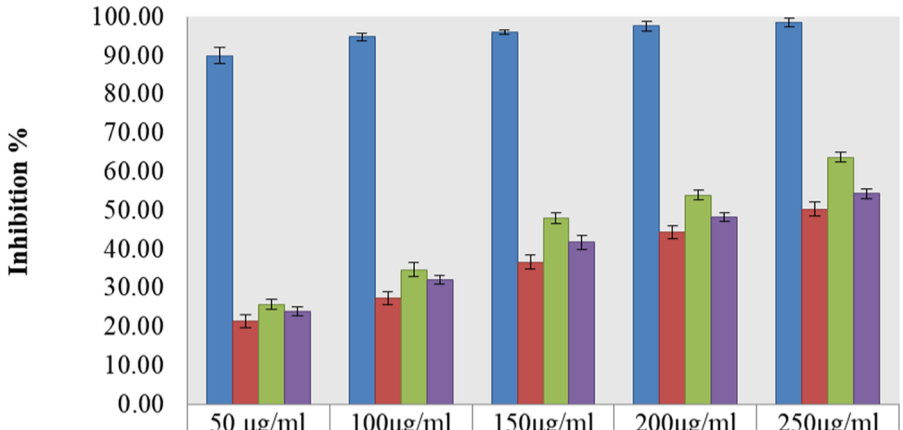

	50 μg/ml	100μg/ml	150μg/ml	200μg/ml	250μg/ml
AA_Scv %	89.98	94.80	96.07	97.58	98.50
AgNP_Scv %	21.38	27.36	36.64	44.35	50.29
AgNP-His_Scv %	25.75	34.67	48.07	53.96	63.76
AgNP-Phen_Scv %	23.92	32.00	41.80	48.17	54.32

Figure 10. Antioxidant activity of the green-synthesized AgNP, AgNP-his, and AgNP-phen using DPPH. AgNP_Scv% refers to the green silver nanoparticle scavenge percentage, AgNP-His_Scv% refers to the green silver nanoparticle functionalized with the histidine scavenge percentage, and AgNP-Phen_Scv% refers to the green silver nanoparticle functionalized with the phenylalanine scavenge percentage.

analysis of the nonfunctionalized AgNP revealed that it is composed of Ag/Ag_2O nanocrystals. The antibacterial and antioxidant activities of the biosynthesized AgNPs were also studied. AgNP-his showed potentially effective antibacterial activities at incredibly low dosages (62.5 μg/mL) against Gram-negative*E. coli* and Gram-positive *S. aureus*, indicating unique physicochemical properties of the AgNP-his. The order of their antioxidant and antibacterial activities was found to be AgNP < AgNP-phen < AgNP-hist. The findings of this study could greatly advance our knowledge about the interaction of AgNP with microbes and further encourage the use of amino acid functionalization as a new tool to design a new generation of potential antibacterial and antioxidant agents.

■ ASSOCIATED CONTENT

Supporting Information

The Supporting Information is available free of charge at https://pubs.acs.org/doi/10.1021/acsomega.3c01910.

Antibacterial activities of AgNPs with 62.5 μg/mL of 2 mM ($AgNO_3$) using the disc diffusion method; mechanism involved in the LALE-based synthesis and characterization of AgNPs; and qualitative phytochemical analysis of *L. abyssinica* leaf extract (PDF)

■ AUTHOR INFORMATION

Corresponding Authors

Gemechu Shumi − *Department of Applied Chemistry, School of Natural Science, Adama Science and Technology University, Adama 1888, Ethiopia*; Email: gameshumi@gmail.com

Taye B. Demissie − *Department of Chemistry, University of Botswana, 00704 Gaborone, Botswana*; orcid.org/0000-0001-8735-4933; Email: demissiet@ub.ac.bw

Tegene Desalegn − *Department of Applied Chemistry, School of Natural Science, Adama Science and Technology University, Adama 1888, Ethiopia*; orcid.org/0000-0003-0239-8326; Email: tegened@yahoo.com

Authors

Rajalakshmanan Eswaramoorthy − *Department of Applied Chemistry, School of Natural Science, Adama Science and Technology University, Adama 1888, Ethiopia; Department of Biomaterials, Saveetha Dental College, and Hospitals, Saveetha Institute of Medical and Technical Sciences, Saveetha University, Chennai 600 077, India*; orcid.org/0000-0002-8331-2100

Raji Feyisa Bogale − *Department of Chemistry, College of Natural and Computational Science, Wollega University, Nekemte 395, Ethiopia*

Girmaye Kenasa − *Department of Biology, College of Natural and Computational Science, Wollega University, Nekemte 395, Ethiopia*

Complete contact information is available at: https://pubs.acs.org/10.1021/acsomega.3c01910

Author Contributions

Experimental: G.S., T.D., and T.B.D.; data analysis: G.S., T.D., T.B.D., R.F.B., and G.K.; methodology: G.S., T.D., and T.B.D.; original draft writing: G.S., T.D., and T.B.D.; and writing—review and editing: G.S., T.D., T. B.D., R.F.B., and G.K.

Notes

The authors declare no competing financial interest.
This study did not include human participants or animals.

■ ACKNOWLEDGMENTS

The authors would like to thank Adama Science and Technology University, Ethiopia, and the University of Botswana for providing research facilities. The authors are also thankful to Chemistry and Biology Departments, Wollega University, Ethiopia, for providing laboratory space to perform the experimental work, UV−Vis spectrophotometry, and antibacterial activity facility.

REFERENCES

(1) Joudeh, N.; Linke, D. Nanoparticle classification, physicochemical properties, characterization, and applications: a comprehensive review for biologists. *J. Nanobiotechnol.* **2022**, *20*, No. 262.

(2) Nadaf, S. J.; Jadhav, N. R.; Naikwadi, H. S.; Savekar, P. L.; Sapkal, I. D.; Kambli, M. M.; Desai, I. A. Green synthesis of Gold and Silver Nanoparticles: Updates on Research, Patents, and Future Prospects. *OpenNano* **2022**, *8*, No. 100076.

(3) Gul, A.; Fozia; Shaheen, A.; Ahmad, I.; Khattak, B.; Ahmad, M.; Ullah, R.; Bari, A.; Ali, S. S.; Alobaid, A.; Asmari, M. M.; Mahmood, H. M. Green synthesis, characterization, enzyme inhibition, antimicrobial potential, and cytotoxic activity of plant mediated silver nanoparticle using *Ricinus communis* leaf and root extracts. *Biomolecules* **2021**, *11*, No. 206.

(4) Sarwer, Q.; Amjad, M. S.; Mehmood, A.; Binish, Z.; Mustafa, G.; Farooq, A.; Qaseem, M. F.; Abasi, F.; de la Lastra, J. M. P. Green Synthesis and Characterization of Silver Nanoparticles Using *Myrsine africana* Leaf Extract for Their Antibacterial, Antioxidant and Phytotoxic Activities. *Molecules* **2022**, *27*, No. 7612.

(5) Hovhannisyan, Z.; Timotina, M.; Manoyan, J.; Gabrielyan, L.; Petrosyan, M.; Kusznierewicz, B.; Bartoszek, A.; Jacob, C.; Ginovyan, M.; Trchounian, K.; Sahakyan, N.; Nasim, M. J. *Ribes nigrum L.* Extract-Mediated Green Synthesis and Antibacterial Action Mechanisms of Silver Nanoparticles. *Antibiotics* **2022**, *11*, No. 1415.

(6) Sivakov, A. G.; Yavetskiy, R. P.; Matveevskaya, N. A.; Beynik, T. G.; Tolmachev, A. V.; Bondarenko, I.; Pokhila, A. S.; Krevsun, A. V.; Koverya, V. P.; Garbuz, A. S. Physica E: Low-dimensional Systems and Nanostructures Study of electrical conductivity of the coatings of bimetallic Au-Ag nanoparticles. *Phys. E* **2020**, *120*, No. 114091.

(7) Lee, S.-B.; Paek, S.; Oh, J. M. Porous Hybrids Structure between Silver Nanoparticle and Layered Double Hydroxide for Surface-Enhanced Raman Spectroscopy. *Nanomaterials* **2021**, *11*, No. 447.

(8) Fathima, R.; Mujeeb, A. Nonlinear optical investigations of laser generated gold, silver and gold-silver alloy nanoparticles and optical limiting applications. *J. Alloys Compd* **2020**, *858*, No. 157667.

(9) Alaqad, K.; Saleh, T. A. Gold, and Silver Nanoparticles: Synthesis Methods, Characterization Routes, and Applications towards Drugs. *J. Environ. Anal. Toxicol.* **2016**, *6*, 1−10.

(10) Naganthran, A.; Gayathiri, V.; Khalid, F. E.; Masarudin, M. J.; Zulkharnain, A.; Nawawi, N. M.; Karim, M.; Abdullah, C. A. C.; Ahmad, S. A. Synthesis, characterization and biomedical applications of silver nanoparticles. *Materials* **2022**, *15*, No. 427.

(11) Gajbhiye, S.; Sakharwade, S. Silver Nanoparticles in Cosmetics. *J. Cosmet., Dermatol. Sci. Appl.* **2016**, *06*, 48−53.

(12) Banerjee, P.; Satapathy, M.; Mukhopahayay, A.; Das, P. Leaf extract mediated green synthesis of silver nanoparticles from widely available Indian plants: Synthesis, characterization, antimicrobial property, and toxicity analysis. *Bioresour. Bioprocess.* **2014**, *1*, No. 3.

(13) Sharma, N. K.; Vishwakarma, J.; Rai, S.; Alomar, T. S.; Almasoud, N.; Bhattarai, A. Green Route Synthesis and Characterization Techniques of Silver Nanoparticles and Their Biological Adeptness. *ACS Omega* **2022**, *7*, 27004−27020.

(14) Samuel, M. S.; Ravikumar, M.; John, A.; Selvarajan, E.; Patel, H.; Chander, P. S.; Soundarya, J.; Vuppala, S.; Balaji, R.; Chandrasekar, N. A Review on Green Synthesis of Nanoparticles and Their Diverse Biomedical and Environmental Applications. *Catalysts* **2022**, *12*, No. 459.

(15) Hieu, H. N.; Trang, D. T. H.; Hien, V. T. T.; et al. Microorganism-mediated green synthesis of silver nanoparticles using *Aspergillus niger* and *Bacillus megaterium*. *Dig. J. Nanomater. Biostruct.* **2022**, *17*, 359−367.

(16) Vishwanath, R.; Negi, B. Conventional and green methods of synthesis of silver nanoparticles and their antimicrobial properties. *Curr. Res. Green Sustainable Chem.* **2021**, *4*, No. 100205.

(17) Gebreslassie, Y. T.; Gebretnsae, H. G. Green and Cost-Effective Synthesis of Tin Oxide Nanoparticles: A Review on the Synthesis Methodologies, Mechanism of Formation, and Their Potential Applications. *Nanoscale Res. Lett.* **2021**, *16*, No. 97.

(18) Alsaiari, N. S.; Alzahrani, F. M.; Amari, A.; Osman, H.; Harharah, H. N.; Elboughdiri, N.; Tahoon, M. A. Plant and Microbial Approaches as Green Methods for the Synthesis of Nanomaterials: Synthesis, Applications, and Future Perspectives. *Molecules* **2023**, *28*, No. 463.

(19) Khandel, P.; Yadaw, R. K.; Soni, D. K.; Kanwar, L.; Shahi, S. K. Biogenesis of metal nanoparticles and their pharmacological applications: present status and application prospects. *J. Nanostruct. Chem.* **2018**, *8*, 217−254.

(20) Remya, R. R.; Julius, A.; Suman, T. Y.; Mohanavel, V.; Karthick, A.; Pazhanimuthu, C.; Samrot, A. V.; Muhibbullah, M. Role of Nanoparticles in Biodegradation and Their Importance in Environmental and Biomedical Applications. *J. Nanomater.* **2022**, *2022*, 1−15.

(21) Soni, V.; Raizada, P.; Singh, P.; Cuong, H. N.; S, R.; Saini, A.; Saini, R. V.; Van Le, Q.; Nadda, A. K.; Le, T.-T.; Nguyen, V.-H. Sustainable and green trends in using plant extracts for the synthesis of biogenic metal nanoparticles toward environmental and pharmaceutical advances: A rev. *Environ. Res.* **2021**, *202*, No. 111622.

(22) Mikhailova, E. O. Silver Nanoparticles: Mechanism of Action and Probable Bio-Application. *J. Funct. Biomater.* **2020**, *11*, No. 84.

(23) Alavi, M.; Kowalski, R.; Capasso, R.; Coutinho, H. D. M.; de Menezes, I. R. A. Various novel strategies for functionalization of gold and silver nanoparticles to hinder drug-resistant bacteria and cancer cells. *Micro Nano. Bio Aspects* **2022**, *1*, 38−48.

(24) Ahmad, F.; Salem-Bekhit, M. M.; Khan, F.; Alshehri, S.; Khan, A.; Ghoneim, M. M.; Wu, H. F.; Taha, E. I.; Elbagory, I. Unique Properties of Surface-Functionalized Nanoparticles for Bio-Application: Functionalization Mechanisms and Importance in Application. *Nanomaterials* **2022**, *12*, No. 1333.

(25) Chakraborty, A.; Boer, J. C.; Selomulya, C.; Plebanski, M. Amino Acid Functionalized Inorganic Nanoparticles as Cutting-Edge Therapeutic and Diagnostic Agents. *Bioconjugate Chem.* **2018**, *29*, 657−671.

(26) Restrepo, C. V.; Villa, C. C. Environmental Nanotechnology, Monitoring & Management Synthesis of silver nanoparticles, influence of capping agents, and dependence on size and shape: A Rev. *Environ. Nanotechnol., Monit. Manage.* **2021**, *15*, No. 100428.

(27) Xu, N.; Chen, G.; Liu, H. Antioxidative categorization of twenty amino acids based on experimental evaluation. *Molecules* **2017**, *22*, No. 2066.

(28) Kumar, M.; Bansal, K.; Gondil, V. S.; Sharma, S.; Jain, D. V. S.; Chhibber, S.; Sharma, R. K.; Wangoo, N. Synthesis, characterization, mechanistic studies and antimicrobial efficacy of biomolecule capped and pH modulated silver nanoparticles. *J. Mol. Liq* **2018**, *249*, 1145−1150.

(29) Sasikumar, J. M.; Erba, O.; Egigu, M. C. In vitro antioxidant activity and polyphenolic content of commonly used spices from Ethiopia. *Heliyon* **2020**, *6*, No. e05027.

(30) Arya, G.; Kumari, R. M.; Gupta, N.; Kumar, A.; Chandra, R.; Nimesh, S. Green synthesis of silver nanoparticles using *Prosopis juliflora* bark extract: reaction optimization, antimicrobial and catalytic activities. *Artif. Cells, Nanomed., Biotechnol.* **2018**, *46*, 985−993.

(31) Ram, S.; Sinha, V. S. Qualitative phytochemical analysis of some plants uses to cure Malaria in Kolhan region, of Jharkhand, India. *J. Med. Plants Stud.* **2015**, *3*, 60−62.

(32) Senguttuvan, J.; Paulsamy, S.; Karthika, K. Phytochemical analysis and evaluation of leaf and root parts of the medicinal herb, *Hypochaeris radicata* L. for in vitro antioxidant activities. *Asian Pac. J. Trop. Biomed.* **2014**, *4*, S359−S367.

(33) Gul, R.; Jan, S. U.; Faridullah, S.; Sherani, S.; Jahan, N. Preliminary Phytochemical Screening, Quantitative Analysis of Alkaloids, and Antioxidant Activity of Crude Plant Extracts from *Ephedra intermedia* Indigenous to Balochistan. *Sci. World J.* **2017**, *2017*, 1−7.

(34) Melkamu, W. W.; Bitew, L. T. Green synthesis of silver nanoparticles using *Hagenia abyssinica* (Bruce) J.F. Gmel plant leaf extract and their antibacterial and anti-oxidant activities. *Heliyon* **2021**, *7*, No. e08459.

https://doi.org/10.1021/acsomega.3c01910
ACS Omega 2023, 8, 24371−24386

(35) Chandra, A.; Singh, M. Biosynthesis of amino acid functionalized silver nanoparticles for potential catalytic and oxygen sensing applications. *Inorg. Chem. Front.* **2018**, *5*, 233−257.
(36) Suresh, S.; Karthikeyan, S.; Jayamoorthy, K. FTIR and multivariate analysis to study the effect of bulk and nano copper oxide on peanut plant leaves. *J. Sci.: Adv. Mater. Devices* **2016**, *1*, 343−350.
(37) Riaz, M.; Sharafat, U.; Zahid, N.; Ismail, M.; Park, J.; Ahmad, B.; Rashid, N.; Fahim, M.; Imran, M.; Tabassum, A. Synthesis of Biogenic Silver Nanocatalyst and their Antibacterial and Organic Pollutants Reduction Ability. *ACS Omega* **2022**, *7*, 14723−14734.
(38) De Zoysa, M. H. N.; Rathnayake, H.; Hewawasam, R. P.; Wijayaratne, W. M. D. G. B. Determination of in Vitro Antimicrobial Activity of Five Sri Lankan Medicinal Plants against Selected Human Pathogenic Bacteria. *Int. J. Microbiol.* **2019**, *2019*, 1−8.
(39) Ali, F.; Younas, U.; Nazir, A.; Hassan, F.; Iqbal, M.; Hamza, B.; Mukhtar, S.; Khalid, A.; Ishfaq, A. Biosynthesis and characterization of silver nanoparticles using strawberry seed extract and evaluation of their antibacterial and antioxidant activities. *J. Saudi Chem. Soc.* **2022**, *26*, No. 101558.
(40) Pandit, C.; Roy, A.; Ghotekar, S.; Khusro, A.; Islam, M. N.; Emran, T. B.; Lam, S. E.; Khandaker, M. U.; Bradley, D. A. Biological agents for synthesis of nanoparticles and their applications. *J. King Saud Univ. Sci.* **2022**, *34*, No. 101869.
(41) Agidew, M. G. Phytochemical analysis of some selected traditional medicinal plants in Ethiopia. *Bull. Natl. Res. Cent.* **2022**, *46*, No. 87.
(42) Belachew, G.; Engeda, D.; Tilku, D. In vitro antioxidant activity of *Lippia adoensis* Var. Koseret, *Thymus schimperi* Ronniger and *Rosmarinus officinalis* Leaf extracts and their effects on oxidative stability of ground raw beef meat during refrigeration storage. *Food Res.* **2022**, *6*, 319−327.
(43) Buli, G. A.; Duga, A. G.; Dessalegn, E. Antimicrobial Activity of *Lippia adoensis* var. koseret Against Human Pathogenic Bacteria and Fungi. *Am. J. Clin. Exp. Med.* **2019**, *3*, 118−123.
(44) Mehata, M. S. Green route synthesis of silver nanoparticles using plants/ginger extracts with enhanced surface plasmon resonance and degradation of textile dye. *Mater. Sci. Eng. B* **2021**, *273*, 1−9.
(45) Purohit, A.; Sharma, R.; Shiv Ramakrishnan, R.; Sharma, S.; Kumar, A.; Jain, D.; Kushwaha, H. S.; Maharjan, E. Biogenic Synthesis of Silver Nanoparticles (AgNPs) Using Aqueous Leaf Extract of *Buchanania lanzan* Spreng and Evaluation of Their Antifungal Activity against Phytopathogenic Fungi. *Bioinorg. Chem. Appl.* **2022**, *2022*, 1−9.
(46) Shaikh, W. A.; Chakraborty, S.; Owens, G.; Islam, R. U. A review of the phytochemical mediated synthesis of AgNP (silver nanoparticle): the wonder particle of the past decade. *Appl. Nanosci.* **2021**, *11*, 2625−2660.
(47) Khalir, W. K. A. W. M.; Shameli, K.; Jazayeri, S. D.; Othman, N. A.; Jusoh, N. W. C.; Hassan, N. M. Biosynthesized Silver Nanoparticles by Aqueous Stem Extract of *Entada spiralis* and Screening of Their Biomedical Activity. *Front. Chem.* **2020**, *8*, 1−15.
(48) Ershov, V.; Tarasova, N.; Ershov, B. Evolution of electronic state and properties of silver nanoparticles during their formation in aqueous solution. *Int. J. Mol. Sci.* **2021**, *22*, No. 10673.
(49) Joy, J.; Gurumurthy, M. S.; Thomas, R.; Balachandran, M. Biosynthesized Ag Nanoparticles: a Promising Pathway for Bandgap Tailoring. *Biointerface Res. Appl.* **2021**, *11*, 8875−8883.
(50) Somee, L. R.; Ghadam, P.; Abdi-Ali, A.; Fallah, S.; Panahi, G. Biosynthesised AgCl NPs using Bacillus sp. 1/11 and evaluation of their cytotoxic activity and antibacterial and antibiofilm effects on multi-drug resistant bacteria. *IET Nanobiotechnol.* **2018**, *12*, 764−772.
(51) Shahzadi, T.; Iqbal, S.; Riaz, T.; Zaib, M. A comparative study based on localized surface plasmon resonance optical characteristics of green synthesized nanoparticles towards spectrophotometric determination of cupric ions. *J. Taibah Univ. Sci.* **2022**, *16*, 912−922.
(52) Meva, F. E.; Segnou, M. L.; Ebongue, C. O.; Ntoumba, A. A.; Kedi, P. B. E.; Deli, V.; Etoh, M. A.; Mpondo, E. M. Spectroscopic synthetic optimizations monitoring of silver nanoparticles formation from *Megaphrynium macrostachyum* leaf extract. *Rev. Bras. Farmacogn.* **2016**, *26*, 640−646.
(53) Manimegalai, S.; Rajeswari, V. D.; Parameswari, R.; Nicoletti, M.; Alarifi, S.; Govindarajan, M. Green synthesis, characterization and biological activity of *Solanum trilobatum*-mediated silver nanoparticles. *Saudi J. Biol. Sci.* **2022**, *29*, 2131−2137.
(54) Al Mashud, M. A.; Moinuzzaman, M.; Hossain, M. S.; Ahmed, S.; Ahsan, G.; Reza, A.; Ratul, R. B. A.; Uddin, M. H.; Momin, M. A.; Jamal, M. A. H. M. Green synthesis of silver nanoparticles using *Cinnamomum tamala* (Tejpata) leaf and their potential application to control multidrug resistant *Pseudomonas aeruginosa* isolated from hospital drainage water. *Heliyon* **2022**, *8*, No. e09920.
(55) Roddu, A. K.; Wahab, A. W.; Ahmad, A.; Taba, P. Green-route synthesis and characterization of the silver nanoparticles resulted by bio-reduction process. *J. Phys.: Conf. Ser.* **2019**, *1341*, No. 032004.
(56) Htwe, Y. Z. N.; Chow, W. S.; Suda, Y.; Mariatti, M. Effect of Silver Nitrate Concentration on the Production of Silver Nanoparticles by Green Method. *Mater. Today: Proc.* **2019**, *17*, 568−573.
(57) Ali, M.; Kim, B.; Bel, K. D.; Norman, D.; Brennan, M.; Shad, G. Green synthesis and characterization of silver nanoparticles using *Artemisia absinthium* aqueous extract— A comprehensive study. *Mater. Sci. Eng. C* **2016**, *58*, 359−365.
(58) Patra, J. K.; Das, G.; Fraceto, L. F.; Campos, E. V. R.; Rodriguez-Torres, M. D. P.; Acosta-Torres, L. S.; Diaz-Torres, L. A.; Grillo, R.; Swamy, M. K.; Sharma, S.; Habtemariam, S.; Shin, H. S. Nano based drug delivery systems: Recent developments and future prospects. *J. Nanobiotechnol.* **2018**, *16*, No. 71.
(59) Zein, R.; Sharrouf, W.; Selting, K. Physical Properties of Nanoparticles That Result in Improved Cancer Targeting. *J. Oncology* **2020**, *2020*, 1−16.
(60) C, K.; S, S.; G, S. M.; S, K. A FTIR approach of green synthesized silver nanoparticles by *Ocimum sanctum* and *Ocimum gratissimum* on mung bean seeds. *Inorg. Nano-Met. Chem.* **2020**, *50*, 606−612.
(61) Oves, M.; Rauf, M. A.; Aslam, M.; Qari, H. A.; Sonbol, H.; Ahmad, I.; Zaman, G. S.; Saeed, M. (2022). Green synthesis of silver nanoparticles by *Conocarpus Lancifolius* plant extract and their antimicrobial and anticancer activities. *Saudi J. Biol. Sci.* **2020**, *29*, 460−471.
(62) Gupta, P.; Rai, N.; Verma, A.; Saikia, D.; Singh, S. P.; Kumar, R.; Singh, S. K.; Kumar, D.; Gautam, V. Green-Based Approach to Synthesize Silver Nanoparticles Using the Fungal Endophyte *Penicillium oxalicum* and Their Antimicrobial, Antioxidant, and In Vitro Anticancer Potential. *ACS Omega* **2022**, *7*, 46653−46673.
(63) Shahzadi, T.; Iqbal, S.; Riaz, T.; Zaib, M. A comparative study based on localized surface plasmon resonance optical characteristics of green synthesized nanoparticles towards spectrophotometric determination of cupric ions. *J. Taibah Univ. Med. Sci* **2022**, *16*, 912−922.
(64) Dharmaraj, D.; Krishnamoorthy, M.; Rajendran, K.; Karuppiah, K.; Annamalai, J.; Durairaj, K. R.; Santhiyagu, P.; Ethiraj, K. Antibacterial and cytotoxicity activities of biosynthesized silver oxide (Ag_2O) nanoparticles using *Bacillus paramycoides*. *J. Drug Delivery Sci. Technol.* **2021**, *61*, No. 102111.
(65) Fayyadh, A. A.; Alzubaidy, M. H. J. Green-synthesis of Ag_2O nanoparticles for antimicrobial assays. *J. Mech. Behav. Mater.* **2021**, *30*, 228−236.
(66) Kayed, K.; Mansour, G. The antimicrobial activity of silver nanoparticles in Ag/Ag_2 O composites synthesized by oxygen plasma treatment of silver thin films. *Curr. Appl. Sci. Technol.* **2022**, *22*, 1439−1449.
(67) Laouini, S. E.; Bouafia, A.; Soldatov, A. V.; Algarni, H.; Tedjani, M. L.; Ali, G. A. M.; Barhoum, A. Green synthesized of ag/ag2o nanoparticles using aqueous leaves extracts of phoenix dactylifera l. And their azo dye photodegradation. *Membranes* **2021**, *11*, No. 468.
(68) Polani, S.; Melamed, S.; Burlaka, L.; De La Vega, F.; Zitoun, D. Large-scale synthesis of polyhedral Ag nanoparticles for printed electronics. *RSC Adv.* **2017**, *7*, 54326−54331.
(69) Giri, A. K.; Jena, B.; Biswal, B.; Pradhan, A. K.; Arakha, M.; Acharya, S.; Acharya, L. Green synthesis and characterization of silver

https://doi.org/10.1021/acsomega.3c01910
ACS Omega 2023, 8, 24371−24386

nanoparticles using *Eugenia roxburghii* DC. extract and activity against biofilm-producing bacteria. *Sci. Rep.* **2022**, *12*, No. 8383.
(70) Anandalakshmi, K.; Venugobal, J.; Ramasamy, V. Characterization of silver nanoparticles by green synthesis method using *Pedalium murex* leaf extract and their antibacterial activity. *Appl. Nanosci.* **2016**, *6*, 399−408.
(71) Alahmad, A.; Feldhoff, A.; Bigall, N. C.; Rusch, P.; Scheper, T.; Walter, J. G. Hypericum perforatum L.-mediated green synthesis of silver nanoparticles exhibiting antioxidant and anticancer activities. *Nanomaterials* **2021**, *11*, No. 487.
(72) Some, S.; Bulut, O.; Biswas, K.; Kumar, A.; Roy, A.; Sen, I. K.; Mandal, A.; Franco, O. L.; İnce, İ. A.; Neog, K.; Das, S.; Pradhan, S.; Dutta, S.; Bhattacharjya, D.; Saha, S.; Das Mohapatra, P. K.; Bhuimali, A.; Unni, B. G.; Kati, A.; Ocsoy, I.; et al. Effect of feed supplementation with biosynthesized silver nanoparticles using leaf extract of *Morus indica* L. V1 on *Bombyx mori* L. (Lepidoptera: Bombycidae). *Sci. Rep.* **2019**, *9*, No. 14839.
(73) Venugopal, K.; Rather, H. A.; Rajagopal, K.; Shanthi, M. P.; Sheriff, K.; Illiyas, M.; Rather, R. A.; Manikandan, E.; Uvarajan, S.; Bhaskar, M.; Maaza, M. Synthesis of silver nanoparticles (Ag NPs) for anticancer activities (MCF 7 breast and A549 lung cell lines) of the crude extract of *Syzygium aromaticum*. *J. Photochem. Photobiol., B* **2017**, *167*, 282−289.
(74) Liaqat, N.; Jahan, N.; Khalil-ur-Rahman; Anwar, T.; Qureshi, H. Green synthesized silver nanoparticles: Optimization, characterization, antimicrobial activity, and cytotoxicity study by hemolysis assay. *Front. Chem.* **2020**, *10*, 1−13.
(75) Wang, L.; Hu, C.; Shao, L. The antimicrobial activity of nanoparticles: present situation and prospects for the future. *Int. J. Nanomed.* **2017**, *12*, 1227−1249.
(76) Kiymaci, M. E.; Erdoğan, H.; Bacanll, M. Antioxidative, cytotoxic, and antibacterial properties of self-assembled glycine-histidine-based dipeptides with or without silver nanoparticles in bio-inspired film. *Arch. Ind. Hyg. Toxicol.* **2022**, *73*, 169−177.

https://doi.org/10.1021/acsomega.3c01910
ACS Omega 2023, 8, 24371−24386